Biomedical Signal Processing and Control 49 (2019) 375–387

Contents lists available at ScienceDirect

Biomedical Signal Processing and Control

journal homepage: www.elsevier.com/locate/bspc

A nonovershooting tracking controller for simultaneous infusion of anesthetics and analgesics☆

Regina Padmanabhan[a], Nader Meskin[a,*], Clara M. Ionescu[b,c,d], Wassim M. Haddad[e]

[a] Department of Electrical Engineering, Qatar University, Qatar
[b] Department of Electrical Energy, Ghent University, Technologiepark 913, 9052 Gent-Zwijnaarde, Belgium
[c] Technical University of Cluj Napoca, Memorandumului Street No. 28, Cluj, Romania
[d] Flanders Make, core lab EEDT, Belgium
[e] School of Aerospace Engineering, Georgia Institute of Technology, Atlanta, GA 30332-0150, USA

ARTICLE INFO

Article history:
Received 8 April 2018
Received in revised form 27 August 2018
Accepted 27 September 2018

Keywords:
Nonovershooting control
Active drug dosing
Biomedical control

ABSTRACT

In this paper, a nonovershooting tracking controller is proposed for the continuous infusion of multiple drugs that have interactive effects. The proposed controller design method exploits the freedom of eigenstructure assignment pertinent to the design of feedback controllers for multi-input, multi-output (MIMO) systems. For drug dosing, a nonovershooting tracking controller restricts the undesirable side effects of drug overdosing. The proposed tracking controller is based on an estimate of the full state using a hybrid extended Kalman filter (EKF) that is used to reconstruct the system states from the measurable system outputs. To illustrate the proposed method, we use one of the common anesthetic and analgesic drug combinations (i.e., propofol and remifentanil) which exhibit nonlinear and synergistic drug interaction. An integral control action is included in the controller design to achieve robust tracking in the presence of patient parameter uncertainty. Simulation results and performance analysis of the proposed control strategy are also presented using 20 simulated patients.

1. Introduction

Critically ill patients in the intensive care units (ICUs) often require fine tuned and long term infusion of anesthetics and analgesics [1]. The term analgesia denotes blunting of pain by medication. In ICUs, sedative and analgesic drugs are used to reduce anxiety, delirium, decrease pain during intubation and extubation, increase patient tolerance after endotracheal tube insertion, and to reduce patient ventilator dysynchrony. Even though the critical task of anesthesia administration has been widely discussed in the literature and studied using clinical trials over the last few decades, several recent reviews on the existing methods highlight various aspects of the problem that needs further research attention [2,3]. Such attempts can help transform the research knowledge in this area into clinically and educationally applicable (bedside) tools [2].

In the case of combined administration of anesthetic and analgesic drugs, the mechanism of action is complex, interlaced, and not yet completely understood making the problem more challenging. There are several factors that influence the pharmacokinetics and pharmacodynamics of a drug in the human body. Patient parameters such as the height, weight, gender, age of the patient, and illnesses associated with the circulation system, renal system, or respiratory system influence the pharmacokinetics and pharmacodynamics of a drug in the patient's body [4–6]. For continuous infusion of anesthetic and analgesic drugs over long periods, it is apparent that an appropriate closed-loop control strategy can be used to enhance patient safety [1,3,5].

Two basic factors to consider while designing a closed-loop controller for anesthesia administration are choosing appropriate parameters for feedback and deciding on a viable control strategy to implement. We use a common sedation assessment measure such as the bispectral index (BIS) to quantify the sedation level of the patient [7,8]. However, when it comes to the assessment of pain levels, a relatively smaller number of measurable variables are identified to quantify the pain levels and thus, facilitate closed-loop control [1,3].

In ICUs, several analgesic drugs are used to suppress the pain sensation and thereby reduce stress. The most reliable and valid indicator of pain is the patient's self-report [1]. However, critically

☆ This publication was made possible by the GSRA Grant No. GSRA1-1-1128-13016 from the Qatar National Research Fund (a member of Qatar Foundation). The findings achieved herein are solely the responsibility of the authors.

* Corresponding author.
E-mail addresses: regina.ajith@qu.edu.qa (R. Padmanabhan), nader.meskin@qu.edu.qa (N. Meskin), ClaraMihaela.Ionescu@UGent.be (C.M. Ionescu), wm.haddad@aerospace.gatech.edu (W.M. Haddad).

https://doi.org/10.1016/j.bspc.2018.09.015
1746-8094/

ill patients are often unable to verbally communicate their level of pain. Other common pain related behaviors and physiological indicators are facial expressions, body movements, lacrimation, sweating, variation in heart rate, mean arterial pressure, and respiratory rate [1,9,10]. The primary hurdle in the design of a closed-loop controller for analgesic administration is the lack of a reliable pain assessment model. In an attempt to identify novel and reliable tools to assess pain, several indices using the electroencephalogram (EEG), electromyogram (EMG), heart rate, respiratory rate, skin conductivity, and facial expression have been proposed [1,11–14].

Closed-loop control of analgesic drugs is addressed in [15] using a fuzzy rule based approach, which makes control decisions based on heart rate variability of the patient to facilitate infusion of the analgesic agent remifentanil. A semi-adaptive controller which relies on the remifentanil induced respiratory depression of the patient for the closed-loop drug titration is proposed in [11]. A model reference adaptive controller and a composite adaptive controller is proposed based on a lower-order model. However, as pointed out in [3], in the case of ICU patients who are supported by mechanical ventilators, respiratory depression may not be a reliable measure to assess analgesic concentration. Furthermore, it is risky to use heart rate and mean arterial pressure as feedback parameters for analgesic titration; this is primarily due to the variation caused by the concomitant infusion of cardiac depressive sedatives or the underlying illness of the patient.

Moreover, in the case of the combined administration of sedatives and analgesics, the controller should take advantage of the synergistic interaction between the drugs to minimize drug dosage [2,16–20]. Several studies point out the association of remifentanil concentration in the blood with muscle activity of a patient [21–25]. In [3], the authors propose a novel electromyogram (EMG)-based surrogate variable to quantify the analgesic level and an extended model predictive control based approach is used to simultaneously derive optimal drug dosing of propofol and remifentanil. The EMG-based analgesic index proposed in [3] relates analgesic concentration to EMG. Given that this variable is suitable for conducting in silico trials and is also measurable, in this paper we use the EMG-based analgesic index to regulate the analgesic drug infusion rate.

Overdosing of anesthetic and analgesic drugs have several side effects such as nausea, hypotension, delayed weaning from mechanical ventilation, immunosuppression, and in certain cases is even fatal for patients [1,2,9]. Moreover, overdosing of anesthetic and analgesic drugs prolongs recovery time, patient stay in hospital, and thus increases treatment costs. In the case of patients in ICUs, anesthetic and analgesic drugs are often required for several hours or days to facilitate cooperative treatment, and it is imperative to avoid drug overdosing. A reliable controller that can be used for anesthesia administration for ICU patients should also be robust in the presence of patient variability [2].

In [26], the authors conduct a benchmark study for the control of hard-disk drive servo systems using the nonovershooting tracking controller that was proposed in [27] and its performance is compared against a wide range of other linear and nonlinear techniques from the literature including proportional-integral-derivative (PID) control, composite nonlinear feedback (CNF) control, and robust and perfect tracking (RPT) control. The controller design method proposed in [27] is also successfully used to implement a nonovershooting tracking controller for a LEGOR® robot [28]. Motivated by the fact that the nonovershooting controller-based method discussed in [27] showed improved performance in terms of faster settling times and less overshoot in benchmark studies, we investigate the applicability of the method to drug dosing control.

As pointed out in [2], in case of continuous infusion of intravenous drugs, tools to continuously measure or accurately predict the plasma concentrations in an individual are not currently available. Hence, in the proposed method, a closed-loop control architecture is developed that relies on measurable outputs such as bispectral index and electromyogram. Moreover, we have added an integrator block in the closed-loop system to address biological patient variability, which can lead to significant differences in patient pharmacokinetics and pharmacodynamics. Control methodologies that regulate drug titration so as to suppress the error between the measured output and the desired output can account for patient variability and address disturbances to a certain extent.

In this paper, we develop a nonovershooting tracking controller for the combined administration of multiple drugs with interactive effects. The proposed controller can track desired outputs such as BIS levels and pain levels without incurring an overshoot in the system response by accounting for the additive, synergistic, and antagonistic drug interaction, and hence, avoiding drug overdosing. Compared to the design strategies proposed for the combined administration of propofol and remifentanil in [3,18,19,29,30], the advantage of the proposed method is its nonovershooting and achieved robustness properties.

The paper is organized as follows. Section 2 presents an introduction to the drug kinetics and dynamics for the disposition of propofol and remifentanil followed by the design of the nonovershooting controller for the simultaneous infusion of these interactive drugs. Simulation results and statistical analysis using the proposed controller for 20 simulated patients are given in Section 3. Limitations of the proposed work and a scope for future research are discussed in Section 4. Conclusions are presented in Section 5.

2. Methods

In this section, we first introduce the mathematical formulation of the pharmacokinetics and pharmacodynamics of the drugs considered and then present the nonovershooting tracking controller design in conjunction with a hybrid extended Kalman filter used to reconstruct an estimate of the system states for feedback.

2.1. Drug disposition model

We use a three-compartment model to represent the drug disposition in the human body, where Compartment 1 models the intravascular blood, Compartment 2 models muscle tissue, and Compartment 3 models fat. An effect-site compartment is also used to account for the drug dynamics at the locus of the drug effect [31]. When infusing several drugs simultaneously, the mass distribution of each drug in the three compartments and the effect-site compartment can be represented using the system states for each drug [32]. We use the superscripts S and A to denote that a given parameter is associated with a sedative or an analgesic drug, respectively.

Since the drug dynamics of a patient varies according to the physiology of the patient, here we use Schnider's drug disposition model that is dependent on patient parameters such as age, weight, etc., as given in [4,29,30,33]. Among the available mathematical models that depict the drug disposition in human body, Schnider's model is one of the key recommended models [32]; this model is currently used clinically to facilitate target controlled infusions [4,34]. The mass balance equations used to model the drug transfer between the various compartments are given by ([30])

$$\begin{aligned}\dot{x}_1(t) &= -(k_{10}^S + k_{12}^S + k_{13}^S)x_1(t) + k_{21}^S \frac{v_2^S}{v_1^S} x_2(t) + k_{31}^S \frac{v_3^S}{v_1^S} x_3(t) + u^S(t),\\ x_1(0) &= x_{10}, \quad t \geq 0,\end{aligned} \tag{1}$$

Table 1
Patient model parameters and equations for the sedative drug propofol and analgesic drug remifentanil [3,30].

Parameter	Sedative	Analgesic	Unit
v_1	4.27	$5.1-0.0201(age-40)+0.072(lbm-55)$	l
v_2	$18.9-0.391(age-53)$	$9.82-0.0811(age-40)+0.108(lbm-55)$	l
v_3	2.38	5.42	l
C_1	$1.89+0.0456(weight-77)-0.681(lbm-59)+0.0264(height-177)$	$2.6-0.0162(age-40)+0.0191(lbm-55)$	$l\,min^{-1}$
C_2	$1.29-0.024(age-53)$	$2.05-0.0301(age-40)$	$l\,min^{-1}$
C_3	0.836	$0.076-0.00113(age-40)$	$l\,min^{-1}$
k_{e0}	0.456	$0.595-0.007(age-40)$	min^{-1}
k_{10}	C_1/v_1	C_1/v_1	min^{-1}
k_{12}	C_2/v_1	C_2/v_1	min^{-1}
k_{13}	C_3/v_1	C_3/v_1	min^{-1}
k_{21}	C_2/v_2	C_2/v_2	min^{-1}
k_{31}	C_3/v_3	C_3/v_3	min^{-1}

$$\dot{x}_2(t) = k_{12}^S \frac{v_1^S}{v_2^S} x_1(t) - k_{21}^S x_2(t), x_2(0) = x_{20}, \tag{2}$$

$$\dot{x}_3(t) = k_{13}^S \frac{v_1^S}{v_3^S} x_1(t) - k_{31}^S x_3(t), x_3(0) = x_{30}, \tag{3}$$

$$\dot{c}_{\text{eff}}^S(t) = k_{e0}^S x_1(t) - k_{e0}^S c_{\text{eff}}^S(t), c_{\text{eff}}^S(0) = c_{\text{eff0}}^S, \tag{4}$$

and

$$\begin{aligned}\dot{x}_4(t) &= -(k_{10}^A + k_{12}^A + k_{13}^A)x_4(t) + k_{21}^A \frac{v_2^A}{v_1^A} x_5(t) + k_{31}^A \frac{v_3^A}{v_1^A} x_6(t) + u^A(t), \\ & x_4(0) = x_{40}, \quad t \geq 0,\end{aligned} \tag{5}$$

$$\dot{x}_5(t) = k_{12}^A \frac{v_1^A}{v_2^A} x_4(t) - k_{21}^A x_5(t), x_5(0) = x_{50}, \tag{6}$$

$$\dot{x}_6(t) = k_{13}^A \frac{v_1^A}{v_3^A} x_4(t) - k_{31}^A x_6(t), x_6(0) = x_{60}, \tag{7}$$

$$\dot{c}_{\text{eff}}^A(t) = k_{e0}^A x_4(t) - k_{e0}^A c_{\text{eff}}^A(t), c_{\text{eff}}^A(0) = c_{\text{eff0}}^A, \tag{8}$$

where $x_i(t)$, $t \geq 0$, $i = 1$, 2, and 3, correspond to the masses of the sedative drug and $x_i(t)$, $t \geq 0$, $i = 4$, 5, and 6, correspond to the masses of the analgesic drug in the first, second, and third compartment, respectively, $c_{\text{eff}}^S(t)$, $t \geq 0$, and $c_{\text{eff}}^A(t)$, $t \geq 0$, denote the effect-site concentrations of the sedative and analgesic drug, respectively, k_{ji}^S and k_{ji}^A, $i \neq j$, denote the rate of mass transfer between the jth and ith compartments, v_i^S and v_i^A, $i = 1$, 2, and 3, are the volume of three compartments, and $u^S(t)$, $t \geq 0$, and $u^A(t)$, $t \geq 0$, are the infusion rates of the sedative and analgesic drug, respectively. Thus, the state vector is given by $x(t) = [x_1(t), x_2(t), x_3(t), c_{\text{eff}}^S(t), x_4(t), x_5(t), x_6(t), c_{\text{eff}}^A(t)]^T$. The values of k_{ji}^S and k_{ji}^A, $i, j = 1$, 2, and 3, in the pharmacokinetic model given by (1)–(8) depend on the patient features such as age, weight, height, and gender, and are given in Table 1.

In Table 1, $lbm = 1.07weight - 148(weight^2/height^2)$, where lbm is the lean body mass of the patient, k_{e0} is the effect-site elimination rate constant, C_1 is the rate at which the drug is cleared from the body by the elimination process, and C_2 and C_3 are the rates of drug clearances between the central compartment and Compartments 2 and 3, respectively. When two drugs with synergistic interactive effects are administrated simultaneously, the effect of each drug varies according to the ratio of the two drugs and their normalized drug concentration. The measured value of the BIS index, denoted as BIS, ranges from 0 to 100, where BIS = 0 and BIS = 100 indicate an isoelectric EEG signal and an EEG signal of a fully conscious patient, respectively.

The net sedative effect of an anesthetic drug when administrated along with an analgesic drug having a synergistic interactive effect is given by ([16])

$$\text{BIS}(t) = \text{BIS}_0 \left(1 - \frac{\left(\frac{U^S(t)+U^A(t)}{U_{50}(\phi(t))} \right)^{\gamma(\phi(t))}}{1 + \left(\frac{U^S(t)+U^A(t)}{U_{50}(\phi(t))} \right)^{\gamma(\phi(t))}} \right), \tag{9}$$

where $\phi(t) \triangleq \frac{U^S(t)}{U^S(t)+U^A(t)}$, $\gamma(\phi(t))$, $t \geq 0$, is the steepness of the concentration-response relation at ratio $\phi(t)$, and $U_{50}(\phi(t))$ is the number of units associated with 50% of maximum effect at ratio $\phi(t)$ [16]. Furthermore, $U^S(t)$, $t \geq 0$, and $U^A(t)$, $t \geq 0$, are the normalized drug concentrations of the sedative and analgesic drugs and are given by $U^S(t) = \frac{c_{\text{eff}}^S(t)}{C_{50}^S}$ and $U^A(t) = \frac{c_{\text{eff}}^A(t)}{C_{50}^A}$, where C_{50}^S and C_{50}^A are the drug concentrations of the sedative and analgesic that cause 50% drug effects, respectively. The BIS value corresponding to fully conscious patient is denoted by BIS_0.

Remifentanil causes pain reduction as well as muscle relaxation [1–3]. Thus, the percentage of muscle relaxation indicates the amount of remifentanil in the blood. We use the EMG index proposed in [3], which relates the effect-site remifentanil concentration to electromyographic measurements. The relationship between the EMG index and remifentanil concentration is given by ([3])

$$\text{EMG}(t) = \frac{100 \times c_{\text{eff}}^A(t)}{3.4 \times c_{\text{eff}}^A(t) + 0.0063}. \tag{10}$$

The value of the EMG(t), $t \geq 0$, indicates the percentage of muscle relaxation and varies from 0% to 100%, and hence, (1)–(10) can be written as

$$\dot{x}(t) = Ax(t) + Bu(t), \quad x(0) = x_0, \quad t \geq 0, \tag{11}$$

$$y(t) = h(x(t)), \tag{12}$$

where $A \in \mathbb{R}^{8\times8}$ is a compartmental matrix [31], $B \in \mathbb{R}^{8\times2}$ is an input matrix, $x(t) \in \mathbb{R}^8$, $t \geq 0$, is the state vector, $u(t) = [u^S(t), u^A(t)]^T$ is the control input, and $y(t) = [\text{BIS}(t), \text{EMG}(t)]^T$ is the system measurement. Here, the initial values of the states x_0 is zero since the masses of the anesthetic and analgesic drugs in all the compartments are zero prior to anesthetic administration.

As shown in the next section, in order to design a nonovershooting controller a linear approximation of the measurements (9) and (10) is required. Using a linear regression model in the region of

the required maintenance value for BIS(t), $t \geq 0$, and EMG(t), $t \geq 0$, (9) and (10) can be represented as ([3,21,29,35])

$$\begin{bmatrix} y_1(t) \\ y_2(t) \end{bmatrix} = \begin{bmatrix} m_1 & m_2 \\ 0 & m_3 \end{bmatrix} \begin{bmatrix} c_{\text{eff}}^{\text{S}}(t) \\ c_{\text{eff}}^{\text{A}}(t) \end{bmatrix} + \begin{bmatrix} c_1 \\ c_2 \end{bmatrix}. \tag{13}$$

The parameter values m_i, $i = 1$, 2, and 3, and the constants c_i, $i = 1$ and 2, in (13) can be determined by multiple linear regression using a least-squares method on randomly selected patient data relating the patient's pharmacokinetic and pharmacodynamic parameters and measured responses [3,29]. Consequently, the linearized patient dynamical model can be written as

$$\dot{x}(t) = Ax(t) + Bu(t), \quad x(0) = x_0, \quad t \geq 0, \tag{14}$$

$$y(t) = Cx(t) + d, \tag{15}$$

where $C = \begin{bmatrix} 0 & 0 & 0 & m_1 & 0 & 0 & 0 & m_2 \\ 0 & 0 & 0 & 0 & 0 & 0 & 0 & m_3 \end{bmatrix}$ and $d = [c_1, c_2]^{\text{T}}$.

2.2. Nonovershooting controller design to achieve target drug effects

In this subsection, we develop a nonovershooting controller design for the control of anesthesia and analgesia. The aim is to design a tracking controller in which the patient responses BIS(t), $t \geq 0$, and EMG(t), $t \geq 0$, asymptotically approach the desired target values $\text{BIS}_{\text{target}}$ and $\text{EMG}_{\text{target}}$ without any overshoot. The key idea behind the nonovershooting controller design is to obtain a state feedback gain that achieves a specific closed-loop eigenstructure such that the selected modes of the closed-loop system appear in each component of the output [36]. In the case of MIMO systems, several choices of state feedback gain matrices lead to the same set of closed-loop eigenvalues but with a different set of eigenvectors [37]. The idea is to exploit this flexibility in a useful way.

Specifically, the closed-loop eigenvectors are selected to achieve a monotonic or nonovershooting response in each output component. In particular, the closed-loop eigenstructure is designed such that the tracking error for each output is driven by a real-valued, closed-loop exponential mode, and hence, each output is monotonic regardless of the initial condition. In cases where it is not possible to restrict the system output to a single mode, the closed-loop eigenstructure is designed to constrain the number of closed-loop modes that appear in each output. However, the output error with multiple modes can remain monotonic for a specific set of initial conditions only.

Motivated by (14) and (15), the proposed nonovershooting controller design method presented is predicated on the linear dynamical system

$$\dot{x}(t) = Ax(t) + Bu(t), \quad x(0) = x_0, \quad t \geq 0, \tag{16}$$

$$y(t) = Cx(t) + d, \tag{17}$$

where, for $t \geq 0$, $x(t) \in \mathbb{R}^n$, $u(t) \in \mathbb{R}^m$, and $y(t) \in \mathbb{R}^p$.

Assumption 1. The pair (A, B) is controllable and the pair (A, C) is observable.

The objective is to design a state feedback controller such that $y(t) \to y_{\text{d}}$ as $t \to \infty$ without any overshoot in the system output. In order to achieve robust tracking in the presence of system parameter uncertainty, an integral control action is included in the controller. We define the integral of tracking error as

$$e(t) = \int_0^t [y_{\text{d}} - y(\tau)]\text{d}\tau, \tag{18}$$

where $y_{\text{d}} = [y_{\text{d1}}, y_{\text{d2}}]^{\text{T}}$ and $y(t) = [y_1(t), y_2(t)]^{\text{T}}$ are the desired response and the measured response, respectively. Note that $\dot{e}(t)$, $t \geq 0$, is given by

$$\dot{e}(t) = y_{\text{d}} - y(t), \quad e(0) = 0, \quad t \geq 0. \tag{19}$$

Furthermore, note that the augmented system Σ_{a} given by (16), (17), and (19) can be written as

$$\begin{aligned} \dot{x}_{\text{a}}(t) &= A_{\text{a}}x_{\text{a}}(t) + B_{\text{a}}u(t) + Gy_{\text{d}} - Hd, \quad x_{\text{a}}(0) = x_{\text{a0}}, \quad t \geq 0, \\ y(t) &= C_{\text{a}}x_{\text{a}}(t) + d, \end{aligned} \tag{20}$$

where $x_{\text{a}}(t) = [x(t), \quad e(t)]^{\text{T}} \in \mathbb{R}^{\hat{n}}$, $\hat{n} = n + p$,

$$A_{\text{a}} = \begin{bmatrix} A & 0 \\ -C & 0 \end{bmatrix}, \quad B_{\text{a}} = \begin{bmatrix} B \\ 0 \end{bmatrix}, \quad G = \begin{bmatrix} 0 \\ I \end{bmatrix}, \quad H = \begin{bmatrix} 0 \\ I \end{bmatrix},$$
$$C_{\text{a}} = [C, \quad 0_{p\times p}]. \tag{21}$$

The aim here is to design a control input $u(t) = K_{\text{a}}x_{\text{a}}(t)$ such that $A_{\text{a}} + B_{\text{a}}K_{\text{a}}$ is asymptotically stable and the output $y(t)$, $t \geq 0$, tracks the reference input y_{d} without any overshoot. Since Σ_{a} is a MIMO system, we can associate multiple sets of $\hat{n}$ eigenvectors for a given set of $\hat{n}$ eigenvalues. We use this flexibility in the eigenvector assignment to achieve the desired nonovershooting property [36]. Specifically, we choose eigenvectors such that a specific set of closed-loop modes appear in the output. Note that for a specific set of $\hat{n}$ eigenvalues $\mathcal{L} = \{\lambda_1, \ldots, \lambda_{\hat{n}}\}$ and linearly independent eigenvectors $\mathcal{V} = \{v_1, \ldots, v_{\hat{n}}\}$, the associated feedback gain matrix K_{a} is unique.

The number of closed-loop modes that can be annihilated from the output signal depends upon the number of invariant zeros of (20) in the open left-half plane (OLHP). For an open-loop system with $\hat{n} - lp$ invariant zeroes in the OLHP, denoted as z_i, $i = 1, \ldots, \hat{n} - lp$, the closed-loop eigenvalues are chosen such that $\lambda_i = z_i$, $i = 1, \ldots, \hat{n} - lp$ [36]. The remaining closed-loop poles λ_i, $i \in \{\hat{n} - lp + 1, \ldots, \hat{n}\}$, can be chosen to be real and asymptotically stable. Finally, for each $i \in \{1, \ldots, \hat{n}\}$, define the Rosenbrock system matrix

$$P_{\Sigma_{\text{a}}} \triangleq \begin{bmatrix} A_{\text{a}} - \lambda_i I & B_{\text{a}} \\ C_{\text{a}} & 0 \end{bmatrix}. \tag{22}$$

Next, let $\mathcal{S} = \{s_1, \ldots, s_{\hat{n}}\} \subset \mathbb{R}^p$, where

$$s_i = \begin{cases} 0, & i \in \{1, \ldots, \hat{n} - lp\}, \\ e_1, & i \in \{\hat{n} - lp + 1, \hat{n} - lp + 2, \ldots, \hat{n} - lp + l\}, \\ \vdots & \vdots \\ e_p, & i \in \{\hat{n} - l + 1, \ldots, \hat{n}\}, \end{cases} \tag{23}$$

and $e_1, \ldots, e_p$ are basis vectors in $\mathbb{R}^p$. Furthermore, assume that, for $1 \leq i \leq \hat{n}$, the matrix equation

$$\begin{bmatrix} A_{\text{a}} - \lambda_i I & B_{\text{a}} \\ C_{\text{a}} & 0 \end{bmatrix} \begin{bmatrix} v_i \\ w_i \end{bmatrix} = \begin{bmatrix} 0 \\ s_i \end{bmatrix} \tag{24}$$

has a solution characterized by $\mathcal{V} = \{v_1, \ldots, v_{\hat{n}}\} \subset \mathbb{C}^{\hat{n}}$ and $\mathcal{W} = \{w_1, \ldots, w_{\hat{n}}\} \subset \mathbb{C}^p$. Now, if the vectors in $\mathcal{V}$ are linearly independent, then there exists a unique feedback gain matrix K_{a} such that, for all $i \in \{1, \ldots, \hat{n}\}$, ([37])

$$\begin{aligned} (A_{\text{a}} + B_{\text{a}}K_{\text{a}})v_i &= \lambda_i v_i, \\ C_{\text{a}}v_i &= s_i. \end{aligned} \tag{25}$$

Now, solving (25) for the vectors in $\mathcal{S}$, we obtain $\mathcal{V} = \{v_1, \ldots, v_{\hat{n}}\}$ and $\mathcal{W} = \{w_1, \ldots, w_{\hat{n}}\}$, where

$$\begin{bmatrix} v_i \\ w_i \end{bmatrix} = \begin{cases} \mathcal{N}(P_{\Sigma_a}(\lambda_i)), & i \in \{1, \ldots, \hat{n} - lp\}, \\ P_{\Sigma_a}^{-1} \begin{bmatrix} 0 \\ s_i \end{bmatrix}, & i \in \{\hat{n} - lp + 1, \ldots, \hat{n}\}, \end{cases} \tag{26}$$

and $\mathcal{N}(\cdot)$ denotes the null space. Thus, vectors in $\mathcal{V}$ satisfy $s_i = C_a v_i$ for all $i = 1, \ldots, \hat{n}$.

If the vectors in $\mathcal{V}$ are linearly independent, then applying Moore's algorithm [37] we obtain K_a as

$$K_a = \mathcal{W}\mathcal{V}^{-1}, \tag{27}$$

where $A_a + B_a K_a$ has distinct eigenvalues corresponding to linearly independent eigenvectors given by $\mathcal{L}$ and $\mathcal{V}$, respectively. The solution $v_i \subset \mathbb{C}^{\hat{n}}$ and $w_i \subset \mathbb{C}^p$ is in the null space of P_{Σ_a} for $s = \lambda_i$, $i = 1, \ldots, \hat{n} - lp$. Now, let $v_{k,1}, v_{k,2}, \ldots, v_{k,l}$ and $\lambda_{k,1}, \lambda_{k,2}, \ldots, \lambda_{k,l}$ be the vectors in $\mathcal{V}$ with their respective eigenvalues associated with the standard basis vector e_k, $k \in 1, \ldots, p$. Note that the desired closed-loop eigenvalues are asymptotically stable and distinct, and hence, can be arranged as $\lambda_{k,1} < \lambda_{k,2} < \cdots < \lambda_{k,l}$, $k \in \{1, \ldots, p\}$.

Since the eigenvalues of the closed-loop system are asymptotically stable, it follows that the tracking error $(y_d - y(t)) \to 0$ as $t \to \infty$. Next, define

$$\hat{A}_a \triangleq A_a + B_a K_a, \qquad \hat{H}_a \triangleq G y_d - H d, \tag{28}$$

so that (20) can be rewritten as

$$\dot{x}_a(t) = \hat{A}_a x_a(t) + \hat{H}_a, \quad x_a(0) = x_{a0}, \quad t \geq 0, \tag{29}$$

$$y(t) = C_a x_a(t) + d. \tag{30}$$

Now, the closed-loop system state of (29) is given by

$$\begin{aligned} x_a(t) &= e^{\hat{A}_a t} x_{a0} + \int_0^t e^{\hat{A}_a (t-\tau)} \hat{H}_a \mathrm{d}\tau \\ &= e^{\hat{A}_a t} x_{a0} + e^{\hat{A}_a t} \int_0^t e^{-\hat{A}_a \tau} \mathrm{d}\tau \hat{H}_a \\ &= e^{\hat{A}_a t} x_{a0} + e^{\hat{A}_a t} \hat{A}_a^{-1} \hat{H}_a - \hat{A}_a^{-1} \hat{H}_a. \end{aligned} \tag{31}$$

Note that the state transition matrix can be written as $e^{\hat{A}_a t} = V e^{\Lambda t} V^{-1}$, where Λ is a diagonal matrix with the eigenvalues λ_i, $i = 1, \ldots, \hat{n}$, on the diagonal and V is a matrix composed of the associated eigenvectors. Thus,

$$x_a(t) = V e^{\Lambda t} V^{-1} x_{a0} + V e^{\Lambda t} V^{-1} \hat{A}_a^{-1} \hat{H}_a - \hat{A}_a^{-1} \hat{H}_a. \tag{32}$$

Now, defining

$$\begin{aligned} \alpha &\triangleq \begin{bmatrix} \alpha_1 & \ldots & \alpha_{n-lp} & \alpha_{1,1} & \ldots & \alpha_{1,l} & \ldots & \alpha_{p,1} & \ldots & \alpha_{p,l} \end{bmatrix}^{\mathrm{T}} \\ &= V^{-1} x_{a0} \end{aligned} \tag{33}$$

and

$$\beta \triangleq V^{-1} \hat{A}_a^{-1} \hat{H}_a, \tag{34}$$

the system output $y(t)$, $t \geq 0$, is given by

$$y(t) = C_a x_a(t) + d = \sum_{i=1}^{\hat{n}} C_a v_i \alpha_i e^{\lambda_i t} + \sum_{i=1}^{\hat{n}} C_a v_i \beta_i e^{\lambda_i t} - \sum_{i=1}^{\hat{n}} C_a v_i \beta_i + d. \tag{35}$$

Since $C_a v_i = s_i$, $i = 1, \ldots, \hat{n}$, (35) gives

$$y(t) = \sum_{i=\hat{n}-lp+1}^{\hat{n}} e_{i-(\hat{n}-lp)} \alpha_i e^{\lambda_i t} + \sum_{i=\hat{n}-lp+1}^{\hat{n}} e_{i-(\hat{n}-lp)} \beta_i e^{\lambda_i t} - \sum_{i=\hat{n}-lp+1}^{\hat{n}} e_{i-(\hat{n}-lp)} \beta_i + d, \tag{36}$$

which implies that $\hat{n} - lp$ terms are annihilated at the system output $y(t)$, $t \geq 0$, and the remaining lp terms are distributed evenly into the p components of $y(t)$, $t \geq 0$, [27]. For the drug dosing model introduced in the previous subsection, we have $\hat{n} = 10$, $l = 3$, and $p = 2$. Moreover, when anesthesia administration begins, the initial drug concentrations in all the compartments are zero. Hence, for $x_{a0} = 0$, $\alpha = 0$, and thus,

$$y(t) = \sum_{i=\hat{n}-3p+1}^{\hat{n}} e_{i-(\hat{n}-lp)} \beta_i e^{\lambda_i t} - \sum_{i=\hat{n}-3p+1}^{\hat{n}} e_{i-(\hat{n}-lp)} \beta_i + d. \tag{37}$$

Now, using Lemma A.2 of [27], we can identify conditions to check the monotonicity of (37). Let $\lambda_1 < \lambda_2 < \lambda_3 < 0$ and define

$$f(t) \triangleq \beta_1 e^{\lambda_1 t} + \beta_2 e^{\lambda_2 t} + \beta_3 e^{\lambda_3 t}. \tag{38}$$

Note that $f(t)$ has a sign change for some $t > 0$ if and only if one of the following conditions holds:

(i) $\beta_1 \beta_2 > 0$, $\beta_1 \beta_3 < 0$, and $|\beta_1 + \beta_2| > |\beta_3|$.
(ii) $\beta_2 \beta_3 > 0$, $\beta_1 \beta_2 < 0$, and $|\beta_1| > |\beta_2 + \beta_3|$.
(iii) (a) $\beta_1 \beta_3 > 0$, $\beta_1 \beta_2 < 0$, and $|\beta_2| \geq |\beta_1 + \beta_3|$;
(b) $\beta_1 \beta_3 > 0$, $\beta_1 \beta_2 < 0$, $|\beta_2| < |\beta_1 + \beta_3|$ and $t^* > 0$, and $|g_c(t^*)| \geq |\beta_1 + \beta_2 + \beta_3|$, where $t^* = \frac{1}{\lambda_3 - \lambda_1} \ln\left(\frac{\beta_1(\lambda_2 - \lambda_1)}{\beta_3(\lambda_3 - \lambda_2)}\right)$ and $g_c(t) = \beta_1(1 - e^{(\lambda_1 - \lambda_2)t}) + \beta_3(1 - e^{(\lambda_3 - \lambda_2)t})$.

Conditions (i)–(iii) give necessary and sufficient conditions under which an output of the form (38) changes sign [27].

Next, in order to design a nonovershooting controller for tracking a desired drug response, we first choose an interval $[a, b]$, where $a, b \in \mathbb{R}$ and $a < b < 0$, and choose $lp = 6$ asymptotically stable and distinct poles. Consider the candidate set $\mathcal{L} = \{\lambda_1, \ldots, \lambda_{\hat{n}}\}$, with lp poles from the interval $[a, b]$ with the remaining $\hat{n} - lp = 4$ poles being the asymptotically stable invariant zeros of Σ_a. Then, solve for $\mathcal{V}$ and β using (26) and (34). If the vectors in the set $\mathcal{V}$ are linearly independent and β is such that none of the Conditions (i)–(iii) are satisfied, then (27) can be used to obtain the feedback control gain K_a; otherwise a new candidate set $\mathcal{L}$ needs to be considered from the interval $[a, b]$. Note that this method does not involve simulating the system response to check for overshoot [27].

Fig. 1 shows the schematic of the proposed nonovershooting controller for the control of simultaneous infusion of an anesthetic and analgesic drug such that the corresponding measurable outputs $\mathrm{BIS}(t)$, $t \geq 0$, and $\mathrm{EMG}(t)$, $t \geq 0$, track the desired targets $y_{d1} \triangleq \mathrm{BIS}_{\mathrm{target}}$ and $y_{d2} \triangleq \mathrm{EMG}_{\mathrm{target}}$, respectively. The method illustrated can be extended to infuse additional drugs provided that the drug effect is linearizable at a given operating point; see Fig. 2.

Even though the aforementioned design is based on the linearized model, the closed-loop is implemented using the measured variables $\mathrm{BIS}(t)$, $t \geq 0$, and $\mathrm{EMG}(t)$, $t \geq 0$, which involves nonlinear functions of the system states. It can be seen from Fig. 2 that the nonlinear measured variables $\mathrm{BIS}(t)$, $t \geq 0$, and $\mathrm{EMG}(t)$, $t \geq 0$, which are given by (9) and (10), can be approximated locally by a linear model. Hence, we use a hybrid extended Kalman filter (EKF) to estimate the system states that are required for state feedback [38,39].

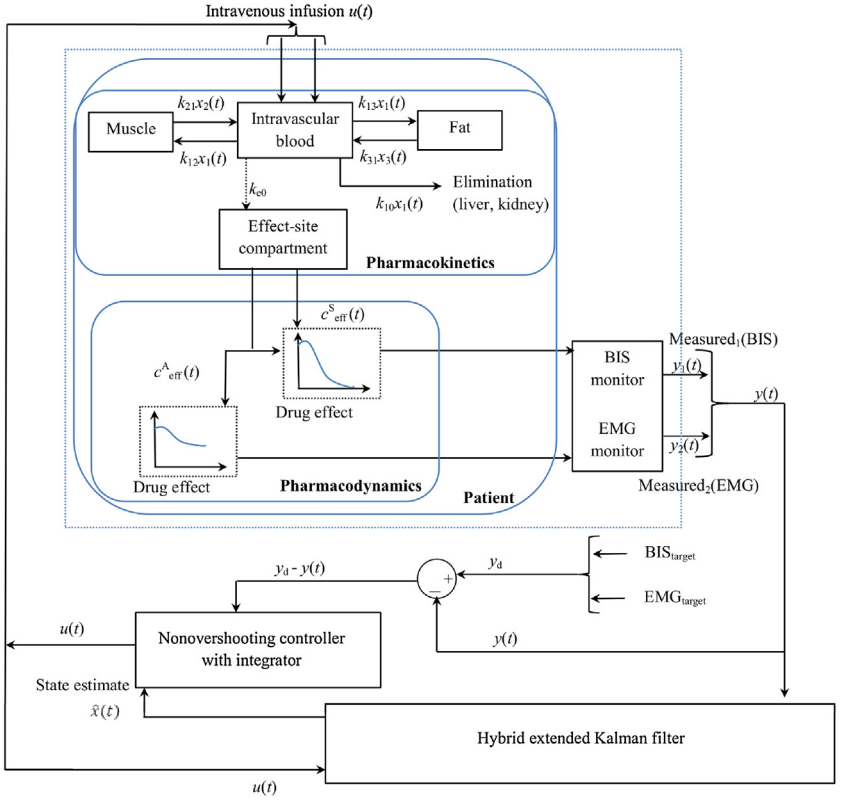

Fig. 1. Closed-loop control for simultaneous drug administration for propofol and remifentanil.

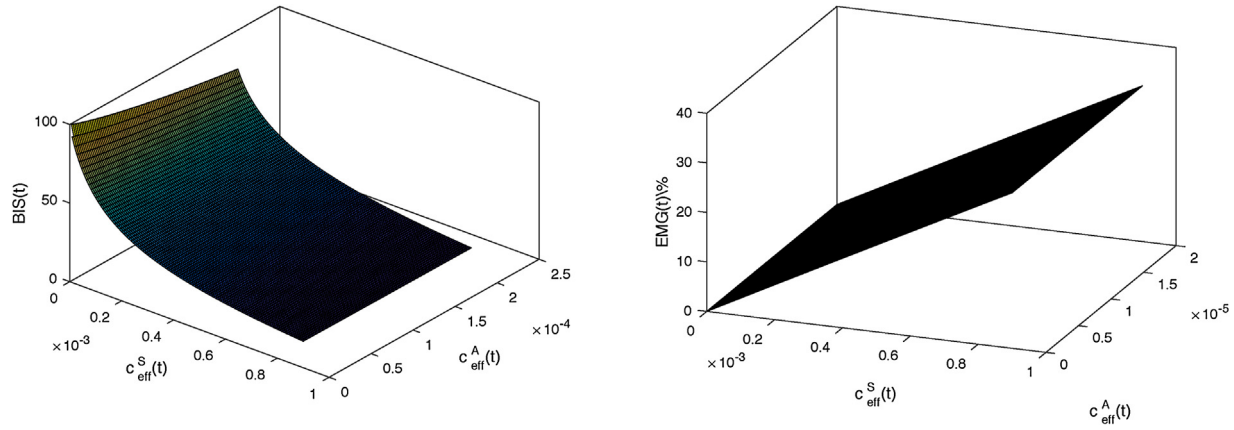

Fig. 2. (a) BIS(t) versus $c^{S}_{eff}(t)$, $t \geq 0$, and $c^{A}_{eff}(t)$, $t \geq 0$. (b) EMG(t)% versus $c^{S}_{eff}(t)$, $t \geq 0$, and $c^{A}_{eff}(t)$, $t \geq 0$, with $C^{S}_{50} = 3.1$ μg/ml, $C^{A}_{50} = 34$ ng/ml, $\gamma(\phi(t)) = 0.9$, and $\theta = 0.22$.

The discrete-time samples of the measured outputs BIS(t), $t \geq 0$, and EMG(t), $t \geq 0$, at the kth time step is given by

$$y_k = [\text{BIS}(x(kT)), \quad \text{EMG}(x(kT))]^{\mathrm{T}}, \quad k = 1, 2, \ldots, \tag{39}$$

where T is the sampling time.

2.3. The hybrid extended Kalman filter [39]

Using the continuous-time dynamics (11) and discrete-time measurement (39) we obtain

$$\dot{x}(t) = Ax(t) + Bu(t) + w(t), \quad x(0) = x_0, \quad t \geq 0, \tag{40}$$

$$y_k = h(x_k) + v_k, \quad k = 1, 2, \ldots, \tag{41}$$

where $x_k = x(kT)$, $w(t)$, $t \geq 0$, denotes a white noise process with intensity $\mathcal{N}(0, Q)$, and v_k, $k = 1, 2, \ldots$, denotes discrete-time white observation noise with covariance $\mathcal{N}(0, R)$.

The hybrid extended Kalman filter for (40) and (41) is given as follows.

(1) Initialize the filter so that

$$\hat{x}_0^{+} = \mathbb{E}[x_0], \tag{42}$$

(2) $Q_{e0}^{+} = \mathbb{E}[(x_0 - \hat{x}_0^{+})(x_0 - \hat{x}_0^{+})^{\mathrm{T}}]$, (43)
where $\mathbb{E}[\cdot]$ denotes expectation.

For $k = 1, 2, \ldots$, perform the following operations.

Table 2
Patient features used to generate simulated patients. Pharmacodynamic parameters of all the 10 patients are set to $C_{50}^{S} = 3.1$ μg/ml, $C_{50}^{A} = 34$ ng/ml, $\gamma(\phi(t)) = 0.9$, and $\theta = 0.22$ [30,33].

Patient No.	*age* [years]	*height* [cm]	*weight* [kg]	*lbm*
1	56	160	88	49.39
2	48	158	52	39.60
3	51	165	55	42.40
4	56	160	65	45.12
5	64	146	60	39.20
6	59	159	110	46.86
7	29	163	59	43.73
8	45	155	58	41.33
9	51	163	55	41.99
10	32	172	56	44.23

1. (a) Integrate the continuous-time model for the state estimate $\hat{x}(t)$, $t \geq 0$, and covariance $Q_e(t)$ as

$$\begin{aligned} \dot{\hat{x}}(t) &= A\hat{x}(t) + Bu(t), \quad (k-1)T \leq t \leq kT, \quad \hat{x}((k-1)T) = \hat{x}_{k-1}^{+}, \\ \dot{Q}_e(t) &= AQ_e(t) + Q_e(t)A^{\mathrm{T}} + Q, \quad (k-1)T \leq t \leq kT, \quad Q_e((k-1)T) = (Q_e)_{k-1}^{+}, \end{aligned} \tag{44}$$

where $\hat{x}_{(k-1)}^{+}$ and $(Q_e)_{(k-1)}^{+}$ are the initial conditions at the beginning of the integration process and at the end of the integration the terminal conditions satisfy $\hat{x}_k^{-} = \hat{x}(kT)$ and $(Q_e)_k^{-} = Q_e(kT)$.

(b) At time instant k, incorporate the measurement y_k into the state estimate and error covariance as

$$K_k = (Q_e)_k^{-} J_k^{\mathrm{T}} (J_k (Q_e)_k^{-} J_k^{\mathrm{T}} + R)^{-1}, \tag{45}$$

$$\hat{x}_k^{+} = \hat{x}_k^{-} + K_k \left(y_k - h(\hat{x}_k^{-}) \right), \tag{46}$$

$$(Q_e)_k^{+} = (I - K_k J_k)(Q_e)_k^{-}, \tag{47}$$

where J_k is the partial derivative of $h(x_k)$ with respect to x_k evaluated at $\hat{x}_k^{-}$.

3. Simulation results

In this section, we present illustrative numerical examples that show the efficacy of the proposed nonovershooting controller design method for the closed-loop control of the simultaneous infusion of anesthetics and analgesics. The simulations are carried out using MATLAB®. For our simulations, we consider two cases. Namely, (1) a design for the controller and observer for each patient using the respective patient model, and (2) a design for the controller and observer using a nominal patient model. For all the simulation results discussed in this section, we set $T = 6$ sec, $R = \begin{bmatrix} 100 & 0 \\ 0 & 0.01 \end{bmatrix}$, $Q = 0.1 I_{8\times 8}$, $\hat{x}_0^{+} = 0$, and $Q_{e0}^{+} = I_{8\times 8}$.

Case 1: First, we consider the pharmacokinetic models of 10 patients obtained using the model (1)–(8) with parameters and patient features given in Tables 1 and 2 , respectively. The pharmacokinetic model of each patient is used to derive the controller gain K_a and estimator gain K_k, $k = 1, 2, \ldots$. Patients in the ICUs often require moderate sedation and analgesia for several hours. Hence, for our simulations, we set the desired target values to $\mathrm{BIS}_{\mathrm{target}} = 60$ and $\mathrm{EMG}_{\mathrm{target}} = 29$ [1,3,31].

The value of the parameters m_i, $i = 1$, 2, and 3, and constants c_i, $i = 1$, and 2, in (13) can be estimated using the multiple linear regression method. The patient response for different combinations of effect-site concentrations $c_{\mathrm{eff}}^{S}(t)$, $t \geq 0$, and $c_{\mathrm{eff}}^{A}(t)$, $t \geq 0$, are obtained using the pharmacodynamic model (9) and (10). For regression, we set the values of the pharmacodynamic parameters to $C_{50}^{S} = 3.1$ μg/ml, $C_{50}^{A} = 34$ ng/ml, and $\gamma(\phi(t)) = 0.9$, and the range of effect-site concentrations to $c_{\mathrm{eff}}^{S}(t) \in [0, \ 30]$ μg/ml and $c_{\mathrm{eff}}^{A}(t) \in [0, \ 25]$ ng/ml. The value of $U_{50}(\phi(t))$, $t \geq 0$, in (9) is calculated using the approximation $U_{50}(\phi(t)) \approx 1 - \theta\phi(t) + \theta\phi^2(t)$, where $\theta = 0.22$ [16]. Using a linear regression, we obtain $m_1 = -1.3263 \times 10^4$, $m_2 = -1.1910 \times 10^6$, $m_3 = 1.5561 \times 10^4$, $c_1 = 84.98$, and $c_2 = 0.0068$. The values of the parameters m_i, $i = 1$, 2, and 3, and the constants c_i, $i = 1$, and 2, can also be estimated by linearizing the system outputs (9) and (10) around the target effect-site concentrations $c_{\mathrm{eff}}^{S_e}$ and $c_{\mathrm{eff}}^{A_e}$, respectively, provided such desired set points for achieving the required value of $\mathrm{BIS}_{\mathrm{target}}$ and $\mathrm{EMG}_{\mathrm{target}}$ are known. To facilitate target controlled infusion (TCI), an estimate of such target effect-site concentrations are calculated by the clinician using the known patient features [4,6].

Using the target effect-site concentrations of propofol and remifentanil $c_{\mathrm{eff}}^{S_e} = 0.7$ μg/ml and $c_{\mathrm{eff}}^{A_e} = 18.18$ ng/ml, respectively, the linearized form of (9) for $\mathrm{BIS}_{\mathrm{target}} = 60$ is given by

$$\begin{aligned} \mathrm{BIS}(c_{\mathrm{eff}}^{S}(t), c_{\mathrm{eff}}^{A}(t)) &= \mathrm{BIS}(c_{\mathrm{eff}}^{S_e}, c_{\mathrm{eff}}^{A_e}) + \left.\frac{\partial \mathrm{BIS}(c_{\mathrm{eff}}^{S}(t), c_{\mathrm{eff}}^{A}(t))}{\partial c_{\mathrm{eff}}^{S}(t)}\right|_{c_{\mathrm{eff}}^{S_e}, c_{\mathrm{eff}}^{A_e}} (c_{\mathrm{eff}}^{S}(t) - c_{\mathrm{eff}}^{S_e}) \\ &\quad + \left.\frac{\partial \mathrm{BIS}(c_{\mathrm{eff}}^{S}(t), c_{\mathrm{eff}}^{A}(t))}{\partial c_{\mathrm{eff}}^{A}(t)}\right|_{c_{\mathrm{eff}}^{S_e}, c_{\mathrm{eff}}^{A_e}} (c_{\mathrm{eff}}^{A}(t) - c_{\mathrm{eff}}^{A_e}) + \mathrm{HOT} \\ &\approx 83 - 1.2403 \times 10^4 c_{\mathrm{eff}}^{S}(t) - 1.07 \times 10^6 c_{\mathrm{eff}}^{A}(t). \end{aligned} \tag{48}$$

Similarly, for $\mathrm{EMG}_{\mathrm{target}} = 29$ and the target effect-site concentration $c_{\mathrm{eff}}^{A_e} = 18.18$ ng/ml, we obtain

$$\begin{aligned} \mathrm{EMG}(c_{\mathrm{eff}}^{A}(t)) &= \mathrm{EMG}(c_{\mathrm{eff}}^{A_e}) + \left.\frac{\partial \mathrm{EMG}(c_{\mathrm{eff}}^{A}(t))}{\partial c_{\mathrm{eff}}^{A}(t)}\right|_{c_{\mathrm{eff}}^{A_e}} (c_{\mathrm{eff}}^{A}(t) - c_{\mathrm{eff}}^{A_e}) + \mathrm{HOT} \\ &\approx 1.5566 \times 10^4 c_{\mathrm{eff}}^{A}(t) + 0.0028. \end{aligned} \tag{49}$$

Note that the value of the parameters m_i, $i = 1$, 2, and 3, and the constants c_i, $i = 1$, and 2, that are obtained using the regression method and linearization given by (48) and (49) are similar.

Even though we use the pharmacological features of the 10 simulated patients given in Table 2 to implement the closed-loop control strategy shown in Fig. 1, for brevity, we present the calculations involved in the design of nonovershooting controller for Patient 1. Using the system dynamics (1)–(8) and (13) we calculate the values of the system matrices A_a, B_a, and C_a. The controllability matrix with respect to the pair (A_a, B_a) has full row rank, and hence, the system is controllable. The stable invariant zeroes z_i, $i = 1, \ldots, \hat{n} - lp$, in the OLHP are calculated using (21), which, for Patient 1, are $z_1 = -0.1986$, $z_2 = -0.0107$, $z_3 - 0.3513$, and $z_4 = -0.0687$. With 4 zeroes in the OLHP, we have $\hat{n} - lp = 4$, where $\hat{n} = 10$, $p = 2$, and $l = 3$.

As discussed in Section 2, we use the asymptotically stable OLHP zeroes of the open-loop system given by z_i, $i = 1, \ldots, 4$, as the desired closed-loop poles of the system, that is, $z_i = \lambda_i$, $i = 1, \ldots, 4$. Given that the system is controllable, we can arbitrarily assign the remaining 6 poles such that the closed-loop system is asymptotically stable. We choose the remaining closed-loop poles to be $\lambda_5 = -0.7125$, $\lambda_6 = -0.5445$, $\lambda_7 = -0.7139$, $\lambda_8 = -0.5510$, $\lambda_9 = -0.4$, and $\lambda_{10} = -0.9$ so that

$$\mathcal{L} = \{z_1, \ldots, z_4, \quad \lambda_5, \ldots, \lambda_{10}\}. \tag{50}$$

Now, using (23), we have $\mathcal{S} = \{s_1, \ldots, s_{10}\}$ given by

$$s_i = \begin{cases} 0, & i \in \{1, \ldots, 4\}, \\ e_1, & i = 5, 6, 7, \\ e_2, & i = 8, 9, 10, \end{cases} \tag{51}$$

that is,

$$\mathcal{S} = \left\{ \begin{bmatrix} 0 \\ 0 \end{bmatrix}, \begin{bmatrix} 0 \\ 0 \end{bmatrix}, \begin{bmatrix} 0 \\ 0 \end{bmatrix}, \begin{bmatrix} 0 \\ 0 \end{bmatrix}, \begin{bmatrix} 1 \\ 0 \end{bmatrix}, \begin{bmatrix} 1 \\ 0 \end{bmatrix}, \begin{bmatrix} 1 \\ 0 \end{bmatrix}, \begin{bmatrix} 0 \\ 1 \end{bmatrix}, \begin{bmatrix} 0 \\ 1 \end{bmatrix}, \begin{bmatrix} 0 \\ 1 \end{bmatrix} \right\}. \tag{52}$$

Table 3
Invariant zeroes in the OLHP for all 10 Patients (Case 1).

Patient No.	Invariant zeroes z_i, $i \in \{1, \ldots, 4\}$
1	−0.1986, −0.0107, −0.3513, −0.0687
2	−0.2416, −0.3513, −0.0676, −0.0124
3	−0.0117, −0.2277, −0.3513, −0.0680
4	−0.0107, −0.2109, −0.0687, −0.3513
5	−0.0090, −0.3513, −0.0703, −0.2160
6	−0.2003, −0.0101, −0.3513, −0.0692
7	−0.2513, −0.0163, −0.0660, −0.3513
8	−0.2399, −0.0130, −0.3513, −0.0673
9	−0.2291, −0.3513, −0.0117, −0.0680
10	−0.2467, −0.0157, −0.0662, −0.3513

Given that $s_i = 0$ for $i \in \{1, \ldots, 4\}$, the corresponding closed-loop mode that is associated with λ_i, $i \in \{1, \ldots, 4\}$, does not appear in the system output.

The eigenvectors in the set $\mathcal{V}$ need to be linearly independent in order to obtain a suitable gain matrix K_a. For any given choice of $\mathcal{L}$ and $\mathcal{S}$, the vectors in the set $\mathcal{V}$ obtained by solving (24) may not be linearly independent. If some of the vectors in the set $\mathcal{V}$, e.g., $\{v_1, \ldots, v_{\hat{n}-3p}\}$ are linearly independent, and some other vectors in the set $\mathcal{V}$, e.g., $\{v_{\hat{n}-3p+1}, \ldots, v_n\}$ are linearly dependent, then one can reorder the p standard basis vectors in $\mathcal{S}$ and resolve (24) to obtain a different set $\mathcal{V}$ [40]. Choosing a different set of closed-loop eigenvalues λ_i, $i = 5, \ldots, 10$, in $\mathcal{L}$ is another option to obtain linearly independent eigenvectors in $\mathcal{V}$.

For the given choice of $\mathcal{L}$ given by (50) and $\mathcal{S}$ given by (52), the vectors in the set $\mathcal{V}$ obtained by solving (24) are linearly independent. Now, substituting the linearly independent eigenvectors in $\mathcal{V}$ obtained by solving (24) in (34) we obtain

$$\begin{aligned}\beta &= \begin{bmatrix} \beta_1 & \beta_2 & \beta_3 & \beta_4 & \beta_{1,1} & \beta_{1,2} & \beta_{1,3} & \beta_{2,1} & \beta_{2,2} & \beta_{2,3} \end{bmatrix}^{\mathrm{T}} \\ &= \begin{bmatrix} 0 & 0 & 0 & 0 & -4.128 \times 10^4 & 446.46 & 4.086 \times 10^4 & 1.9619 & -1.8864 & -0.3627 \end{bmatrix}^{\mathrm{T}}. \end{aligned} \tag{53}$$

Finally, to check the system output for sign changes, we consider the exponential term in (37) given by $\sum_{i=\hat{n}-3p+1}^{\hat{n}} e_{i-(\hat{n}-lp)} \beta_i e^{\lambda_i t}$ and use (53) to define

$$\begin{bmatrix} \beta_{1,1} e^{\lambda_{1,1}} + \beta_{1,2} e^{\lambda_{1,2}} + \beta_{1,3} e^{\lambda_{1,3}} \\ \beta_{2,1} e^{\lambda_{2,1}} + \beta_{2,2} e^{\lambda_{2,2}} + \beta_{2,3} e^{\lambda_{2,3}} \end{bmatrix} \triangleq \begin{bmatrix} f_1(t) \\ f_2(t) \end{bmatrix}. \tag{54}$$

Note that $f_i(t)$, $i = 1$ and 2, is in the form of (38). Now, it can be easily verified that none of the Conditions (i)–(iii) are met for $f_1(t)$, $t \geq 0$, and $f_2(t)$, $t \geq 0$, with β given by (53), and hence, (54) does not possess any sign changes implying that system output (37) is monotonic. Note that we do not have to obtain the response of the system to verify whether the Conditions (i)–(iii) are satisfied. Using the values of K_a and β, one can check whether the system output (37) meets the conditions for a nonovershooting response.

Similar calculations are performed for Patients 2 through 10. The stable invariant zeroes in the OLHP are calculated using (21) for each patient and are given in Table 3. Note that we choose the remaining closed-loop poles to be $\lambda_5 = -0.7125$, $\lambda_6 = -0.5445$, $\lambda_7 = -0.7139$, $\lambda_8 = -0.5510$, $\lambda_9 = -0.4$, and $\lambda_{10} = -0.9$ for Patients 1 through 10.

Figs. 3–5 show the simulation results when the proposed nonovershooting controller is used for the simultaneous infusion of propofol and remifentanil. We use the patient parameters given in Table 1 along with the model equations given in Table 2, (1)–(8), and (13) to derive the respective controller gain K_a and estimator gain K_k, $k = 1, 2, \ldots$, for each of the 10 patients. Note that although the controller is designed based on the approximated linear pharmacodynamic model given by (13), we use the nonlinear pharmacodynamic model given by (9) and (10) for the simulations.

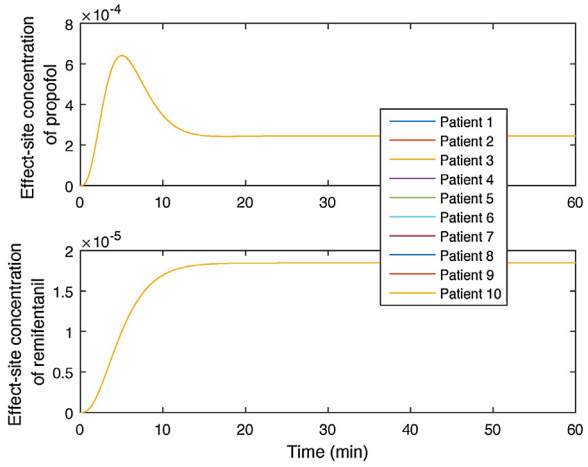

Fig. 3. Drug concentrations in the effect-site for the 10 patients (Case 1).

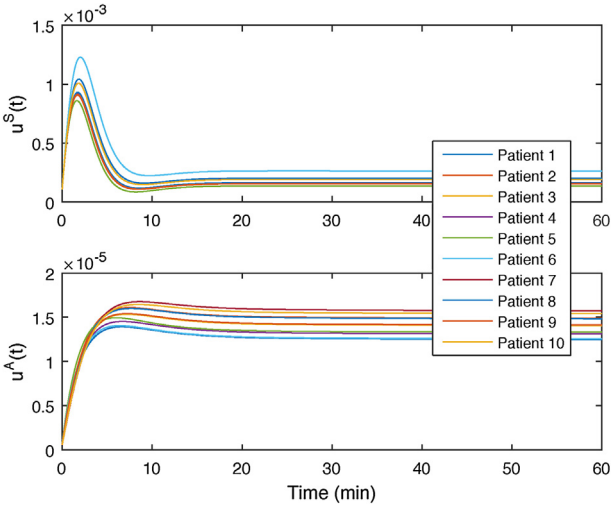

Fig. 4. Control inputs versus time for the 10 patients (Case 1).

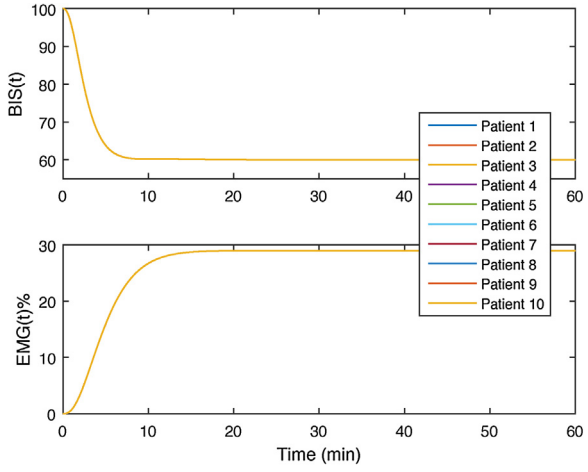

Fig. 5. Drug responses versus time for the 10 patients for $BIS_{target} = 60$ and $EMG_{target} = 29$ (Case 1).

It is clear from Figs. 3–5 that the responses of all 10 patients are monotonic without any overshoot. It can be seen from Fig. 5 that all 10 patients have similar responses due to the fact that the closed-loop poles λ_i, $i = 5, \ldots, 10$, are chosen to be the same for all the 10 patients. Moreover, since the pharmacodynamic parameters

Table 4
Patient features and pharmacodynamic parameters [30,33,43].

No.	*age* [years]	*height* [cm]	*weight* [kg]	C_{50}^{S} [μg/ml]	C_{50}^{A} [ng/ml]	$\gamma(\phi(t))$	θ
11	56	160	88	3.1	34	0.9	0.22
12	48	158	52	2	34	0.8	0.3
13	29	163	59	4	33	0.9	0.22
14	64	146	90	2	39.4	0.8	0.15
15	68	158	113	4	39	0.9	0.22
16	50	161	68	3.1	34	0.9	0.22
17	68	160	88	3.1	34	0.7	0.1
18	70	161	78	3	32	0.8	0.20
19	73	162	75	3.2	34	0.9	0.21
20	45	155	58	3	33	0.85	0.22

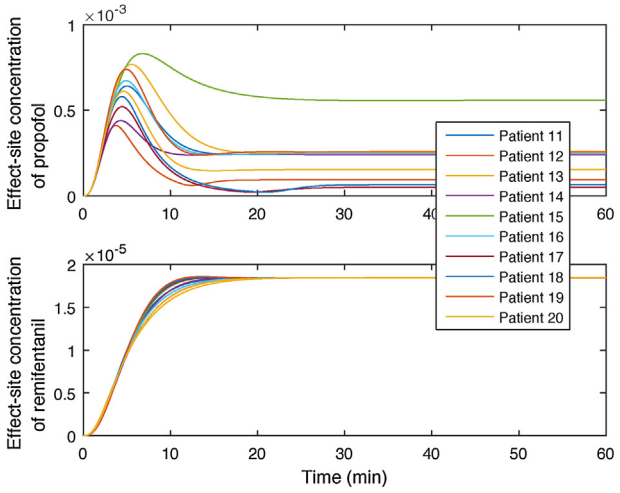

Fig. 6. Drug concentrations in the effect-site for the 10 patients (Case 2).

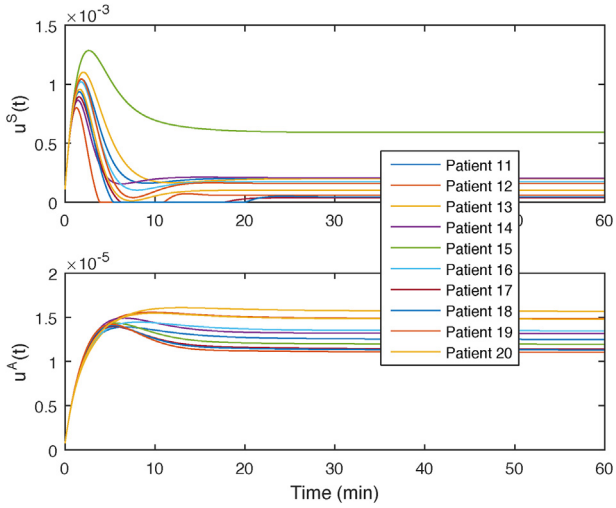

Fig. 7. Control inputs versus time for the 10 patients (Case 2).

for all the 10 patients are assumed to be the same (see Table 2), the values of the effect-site concentrations $c_{\text{eff}}^{S}(t)$, $t \geq 0$, and $c_{\text{eff}}^{A}(t)$, $t \geq 0$, that are required to track a given value of $\text{BIS}_{\text{target}}$ and $\text{EMG}_{\text{target}}$, respectively, are the same for all the patients; see Fig. 3. However, due to the difference in the patient physiological features, the pharmacokinetic parameters are different, and hence, the control input that is required to achieve a certain effect-site concentration is different for each patient; see Fig. 4. It can be seen that out of the 10 patients mentioned in Table 2, Patient 6, with the highest weight and second highest value of lean body mass, requires the highest amount of propofol to achieve the required effect-site concentration. Similarly, Patient 5, who has the least value of lean body mass, requires the least amount of propofol to achieve the required effect-site concentration.

Case 2: In order to analyze the robustness of the nonovershooting controller to pharmacokinetic and pharmacodynamic variability from the nominal model (Patient 1), we consider 10 patients with parameters given in Table 4. We use the controller gain K_a and estimator gain K_k, $k = 1, 2, \ldots$, derived using the pharmacokinetic and pharmacodynamic model of Patient 1 to control the continuous infusion of propofol and remifentanil in Patients 11 through 20. In order to ensure that the infusion rates are nonnegative, we use the control input $u(t) = \max\{0, u(t)\}$, $t \geq 0$.

Figs. 6–8 show the responses of the 10 patients with different pharmacokinetic and pharmacodynamic parameters. It can be seen from Fig. 6 that the effect-site concentration of propofol and remifentanil required to achieve the target values of $\text{BIS}_{\text{target}} = 60$ and $\text{EMG}_{\text{target}} = 29$ for Patients 11 through 20 are considerably different as compared to that of the nominal model used for the controller design; see Fig. 3. This is due to the fact that the pharmacodynamics of Patients 11 through 20 are significantly different between patients, whereas for Patients 1 through 10 the pharmacodynamic parameters are assumed to be the same. Moreover, note that the controller is designed based on the approximated linear pharmacodynamic model given by (13). Hence, Figs. 6–8 show an achieved robustness of the proposed nonovershooting controller with respect to interpatient variability.

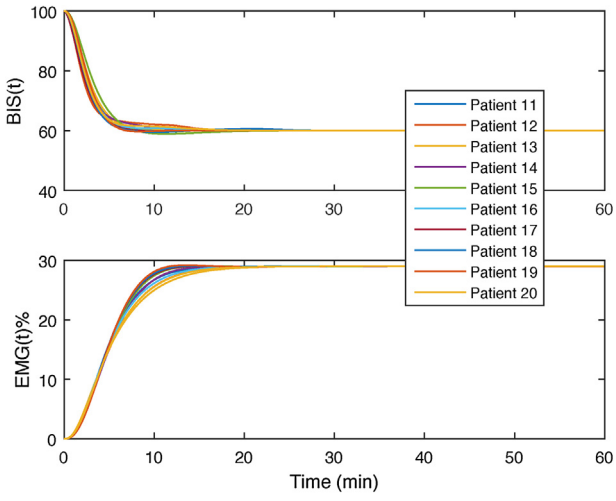

Fig. 8. Drug responses versus time for the 10 patients for $\text{BIS}_{\text{target}} = 60$ and $\text{EMG}_{\text{target}} = 29$ (Case 2).

Next, to quantify the performance of the proposed nonovershooting controller for closed-loop control of multiple drugs, we present statistical analysis based on the simulation results presented in Figs. 6–8 . To do this, recall that anesthesia administration involves an induction phase, in which the patient state is driven

close to the target state, and a maintenance phase, in which the patient state is required to follow the target state. Different performance measures have been suggested in the literature to evaluate the controller performance during these two phases [41,42].

To quantify the performance of the proposed closed-loop control strategy, we can use the median performance error (MDPE), median absolute performance error (MDAPE), root mean square error (RMSE), interquartile range (IQ), minimum and maximum values of the controlled variable (min-max), induction duration (ID), percentage undershoot (US), and percentage overshoot (OS) [41] [42]. Among the listed performance measures, the induction duration, percentage undershoot, and percentage overshoot are the metrics used to analyze the transience during the initial induction phase of anesthesia administration.

The instantaneous performance error (PE) is defined as

$$\mathrm{PE}_i(j) \triangleq \frac{\text{Measured Value}_i(j) - \text{Target Value}}{\text{Target Value}} \times 100, \quad j = 1, \ldots, N, \tag{55}$$

where $i \in \{1, \ldots, 10\}$ represents the ith patient, j represents the set of PE measurements for an individual, N is the number of measurements for each patient, and Measured Value and Target Value refer to the measured and target values of the BIS and EMG, respectively. The median performance error (MDPE) gives the output bias observed and is computed by

$$\mathrm{MDPE}_i = \mathrm{median}(\mathrm{PE}_i(j)), \qquad j = 1, \ldots, N, \tag{56}$$

whereas

$$\mathrm{MDAPE}_i = \mathrm{median}(|\mathrm{PE}_i(j)|), \qquad j = 1, \ldots, N, \tag{57}$$

and

$$\mathrm{RMSE}_i = \sqrt{\frac{\sum_{j=1}^{N}(\text{Measured Value}_i(j) - \text{Target Value})^2}{N}}. \tag{58}$$

MDAPE_i is the median absolute performance error and reflects the size of the error and the accuracy of the controller in maintaining the controlled variables BIS and EMG for each patient [41,42]. RMSE_i represents the standard deviation between the target value and measured values of the controlled variables for each patient.

Induction phase duration (ID) is the time elapsed from the start of drug administration to the time when the drug effect falls to and remains within the range of target values $\mathrm{BIS}_{\mathrm{target}} \pm 10$ and $\mathrm{EMG}_{\mathrm{target}} \pm 3$ for 30 seconds. Percentage undershoot (US) is defined for the controlled variable BIS as ([41])

$$\mathrm{US}_i = \max_j \left(\frac{\mathrm{BIS}_{\mathrm{target}} - \mathrm{BIS}_i(j)}{\mathrm{BIS}_0 - \mathrm{BIS}_{\mathrm{target}}} \right) \times 100, \quad j = 1 \ldots, N, \tag{59}$$

and percentage overshoot (OS) is defined for the controlled variable EMG as

$$\mathrm{OS}_i = \max_j \left(\frac{\mathrm{EMG}_i(j) - \mathrm{EMG}_{\mathrm{target}}}{\mathrm{EMG}_{\mathrm{target}}} \right) \times 100, \quad j = 1 \ldots, N. \tag{60}$$

The variation in the induction phase duration in Figs. 6–8 is mainly due to the mismatch in the pharmacokinetic and pharmacodynamic values of the 10 patients compared to the nominal model (Patient 1) that is used for the controller design. Table 5 shows the performance metrics of the proposed nonovershooting controller for the controlled variables BIS and EMG. In this table, the range of values of the defined performance metrics are given for Patients 11 through 20 (Case 2). Note that the amount of inaccuracy that is reflected in the values of the performance metrics for the 10 patients are within the acceptable performance range [3,41,42,44–46]. The minimum and maximum ranges of the BIS value and EMG value are within $\mathrm{BIS}_{\mathrm{target}} \pm 10$ and $\mathrm{EMG}_{\mathrm{target}} \pm 3$,

Table 5
Performance metrics for controlled variables BIS and EMG (Case 2).

Performance metrics (for 10 patients)	Controlled variables	
	BIS	EMG
MDPE [%]	-0.0090 ± 0.0085	0.0027 ± 0.0329
MDAPE [%]	2.817 ± 0.48	7.87 ± 0.48
Min–Max	58.95–63.12	25.99–29.22
Interquartile Range	0.029	0.0001
RMSE	4.91 ± 0.48	0.050 ± 0.0006
ID [min]	4 ± 0.6	9.3 ± 1.2
US/OS [%]	0–2.625	$0 - 0.75$

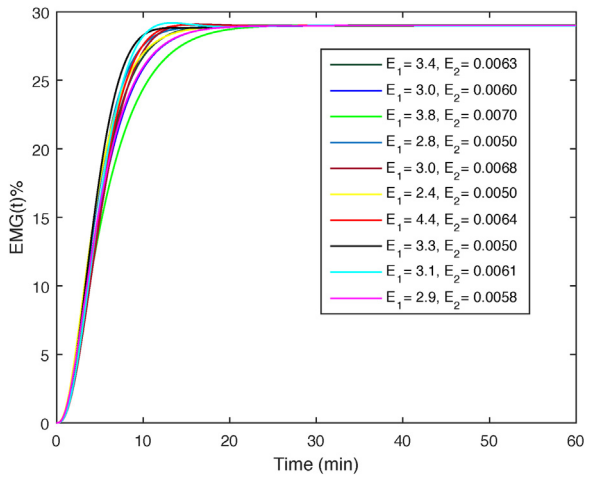

Fig. 9. EMG(t) versus time for the 10 patients with parameter variations in E_1 and E_2 for $\mathrm{EMG}_{\mathrm{target}} = 29$ (Case 2).

respectively. We have also listed the interquartile range, which shows the central tendency of the measured variables for the 10 simulated patients. The interquartile range shows the variability in the middle 50% of a sorted data set.

Note that for the simulations presented in Figs. 6–8 the pharmacodynamic model parameter values of the EMG index in (10) are assumed to be the same for all the 10 patients. These model parameter values can be patient sensitive and should be considered to check the achieved robustness of the controller. However, there is no data available in the literature regarding the possible range of parameter variations. Hence, we simulated the patient responses for the arbitrary parameter values of $E_1 = 3.4 \pm 1$ and $E_2 = 0.0063 \pm 0.0013$ in

$$\mathrm{EMG}(t) = \frac{100 \times c_{\mathrm{eff}}^{\mathrm{A}}(t)}{E_1 \times c_{\mathrm{eff}}^{\mathrm{A}}(t) + E_2}. \tag{61}$$

Fig. 9 shows the simulation results using the simulated Patients 11 through 20 with different pharmacodynamic parameter values in (61). For the 10 patients, we obtain MDPE = -0.0069 ± 0.049, MDAPE = 7.7451 ± 1.01, and ID = 10.05 ± 2.05. Furthermore, during the 60 min drug infusion, the maximum value of EMG response for all the 10 patients is EMG = 29.20%, which corresponds to an overshoot of 0.69%. All these performance metrics are within the acceptable range given in [3,46]. However, it can be seen from Fig. 9 that the induction phase duration for some patients has increased considerably. This may be due to the wide range of parameter variations that are used. Further research is required to validate the adequacy of the range of model parameter variations.

Finally, in order to further investigate whether adequate analgesia is achieved, we use other pharmacodynamic models that account for the patient response with respect to various clinically relevant painful stimuli and the drug concentrations in the effect-

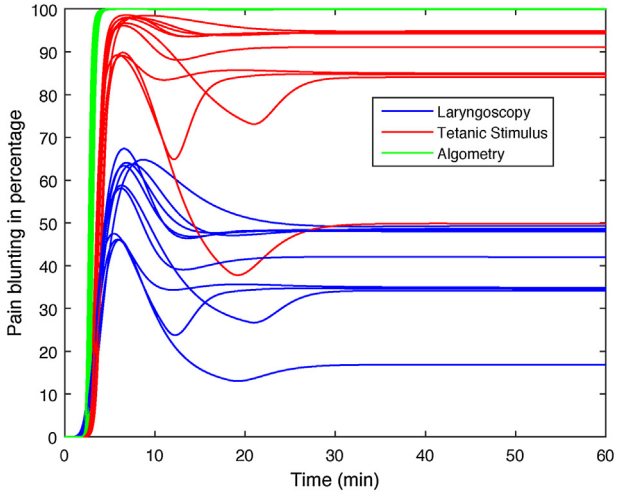

Fig. 10. Response to three painful stimuli for the 10 patients with $BIS_{target} = 60$ and $EMG_{target} = 29$.

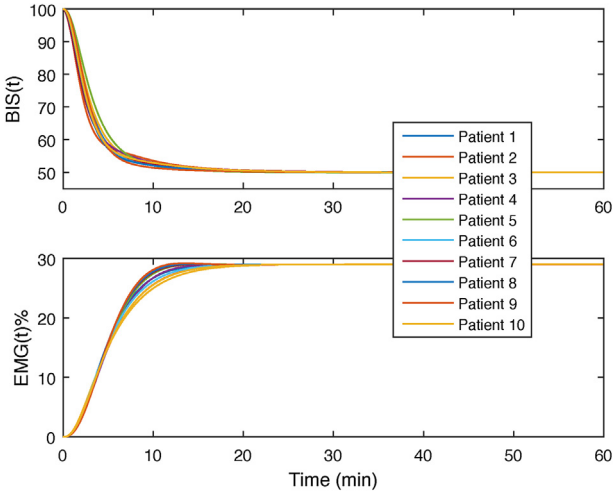

Fig. 11. Drug responses versus time for the 10 patients $BIS_{target} = 50$ and $EMG_{target} = 29$.

site. Note that in case of the combined administration of anesthetics and analgesics, the drug concentrations C_{50}^{S} and C_{50}^{A} that cause 50% analgesic effect vary considerably with respect to the intensity of the painful stimuli [9].

In [47], the authors provide response surface models with respect to blunting of pain for the combined administration of the drugs propofol and remifentanil. Specifically, Grego interaction models that account for the painful stimuli involved in clinical procedures such as the pressure algometry, tetanic stimulation, and laryngoscopy are given as ([47])

$$\text{Effect}_{\text{Algometry}}(t) = \frac{\left(\frac{c_{\text{eff}}^{S}(t)}{4.16} + \frac{c_{\text{eff}}^{A}(t)}{8.84} + 8.2 \times \frac{c_{\text{eff}}^{S}(t)}{4.16} \times \frac{c_{\text{eff}}^{A}(t)}{8.84}\right)^{8.34}}{\left(\frac{c_{\text{eff}}^{S}(t)}{4.16} + \frac{c_{\text{eff}}^{A}(t)}{8.84} + 8.2 \times \frac{c_{\text{eff}}^{S}(t)}{4.16} \times \frac{c_{\text{eff}}^{A}(t)}{8.84}\right)^{8.34} + 1}, \tag{62}$$

$$\text{Effect}_{\text{Tetanic stimulus}}(t) = \frac{\left(\frac{c_{\text{eff}}^{S}(t)}{4.57} + \frac{c_{\text{eff}}^{A}(t)}{21.3} + 14.7 \times \frac{c_{\text{eff}}^{S}(t)}{4.57} \times \frac{c_{\text{eff}}^{A}(t)}{21.3}\right)^{6.0}}{\left(\frac{c_{\text{eff}}^{S}(t)}{4.57} + \frac{c_{\text{eff}}^{A}(t)}{21.3} + 14.7 \times \frac{c_{\text{eff}}^{S}(t)}{4.57} \times \frac{c_{\text{eff}}^{A}(t)}{21.3}\right)^{6.0} + 1}, \tag{63}$$

$$\text{Effect}_{\text{Laryngoscopy}}(t) = \frac{\left(\frac{c_{\text{eff}}^{S}(t)}{5.6} + \frac{c_{\text{eff}}^{A}(t)}{48.9} + 33.2 \times \frac{c_{\text{eff}}^{S}(t)}{5.6} \times \frac{c_{\text{eff}}^{A}(t)}{48.9}\right)^{2.2}}{\left(\frac{c_{\text{eff}}^{S}(t)}{5.6} + \frac{c_{\text{eff}}^{A}(t)}{48.9} + 33.2 \times \frac{c_{\text{eff}}^{S}(t)}{5.6} \times \frac{c_{\text{eff}}^{A}(t)}{48.9}\right)^{2.2} + 1}. \tag{64}$$

Since such stimuli are commonly used in the ICU for patient assessment, we use the pharmacodynamic models (62)–(64) to investigate whether adequate anesthesia and analgesia is achieved when the nonovershooting controller is used for the control of propofol and remifentanil to achieve $BIS_{target} = 60$ and $EMG_{target} = 29$ [48].

Fig. 10 shows the response of the Patients 11 through 20 for the three painful stimuli given in (62)–(64). Note that we do not regulate the infusion of propofol and remifentanil with respect to these responses. Fig. 10 is plotted to examine whether adequate pain blunting is achieved when we use the BIS and EMG as the controlled variables. It can be seen that adequate pain blunting (greater than 90%) is achieved for all the 10 patients with respect to the painful stimuli involved in pressure algometry. In case of tetanic stimuli, 7 out of the 10 patients show adequate analgesia. Note that, as depicted by (62)–(64), the patient response to painful stimuli depends on the values of $c_{\text{eff}}^{S}(t), t \geq 0$, and $c_{\text{eff}}^{A}(t), t \geq 0$. As we have set $BIS_{target} = 60$, which indicates a moderate sedation level, all the 10 patients show less than 70% tolerance to laryngoscopy. Deeper sedation is recommended to facilitate clinical procedures such as laryngoscopy, which involves more pain intensity [49].

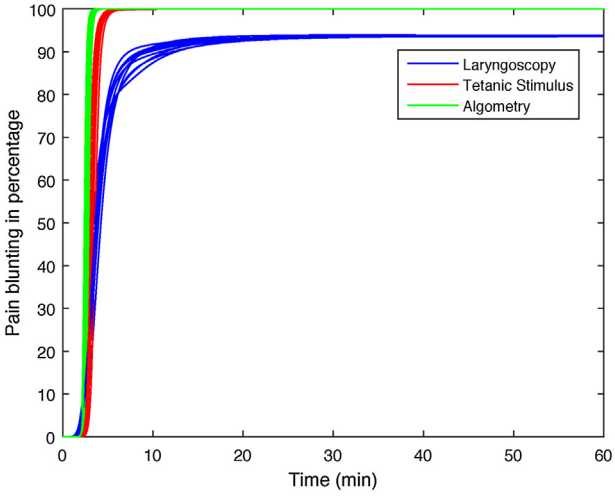

Fig. 12. Response to three painful stimuli for the 10 patients with $BIS_{target} = 50$ and $EMG_{target} = 29$.

Figs. 11 and 12 show the response of the simulated Patients 11 through 20 using the nominal patient model with a deeper sedation target set at $BIS_{target} = 50$. In this case, it can be seen that all the patients show adequate tolerance to laryngoscopy stimulus. Moreover, compared to Fig. 10, it can be seen from Fig. 12 that the time taken to achieve an adequate level of pain tolerance is reduced considerably for all the three painful stimuli.

4. Discussion

In undersedation, the patient's level of consciousness depends mainly on the concentration of the sedative drug in the effect-site. However, in inadequate analgesia, the level of pain sensation depends mainly on three factors; the concentration of the analgesic drug in the effect-site, the strength of the painful stimuli, and the

endogenous pain reduction mechanisms [13,16,43]. Another discrepancy is that the analgesic requirement should be high while the stimuli is present and moderate afterwards. Unlike the operating room, in the intensive care units analgesic titration should be raised during intubation or extubation and should be moderate when the patient remains intubated. It should be noted that the increased drug titration is required before the application of stimulus, and it is futile to sense inadequate analgesia and titrate more drugs when the actual painful stimuli no longer exists.

Furthermore, we have not analyzed whether restricting the drug titration so as to avoid overshoot with respect to sedation and analgesia has helped to keep the hemodynamic parameters of the patient within safe limits. Apart from variation in cardiovascular parameters, analgesics show dose dependent effect on respiration [11]. Response surface modeling of separate and combined administration of propofol and remifentanil reveals that their effect on respiration is strikingly synergistic. Thus, titration of analgosedatives to the critically ill patients must be regulated to maintain respiratory rate within safe limits.

Typically, anesthetic and analgesic drugs are administrated on a continuous or scheduled intermittent basis, with supplemental bolus doses as required [1]. Both propofol and remifentanil are short acting drugs and have rapid onset time [1,9]. As noted in [1] and [9], for drugs with very short duration of action, continuous infusion is recommended. It can be seen from Figs. 4 and 7 that, similar to the typical dosing regimen that is used during anesthesia administration, the proposed controller is able to derive a control input with an initial high dose that resembles a bolus dose to induce anesthesia and then a constant drug dose to maintain the required target levels of drug responses.

The proposed nonovershooting controller design strategy is particularly attractive for the control of anesthesia administration as it involves infusion of multiple drugs to achieve several targeted effects. Often anesthesia administration involves concomitant administration of two or more anesthetics, analgesics, neuromuscular blockades, anticholinergics, and colloid and crystalloid fluids so as to achieve desired drug effects such as sedation level, pain blunting, muscle relaxation, reduced organ secretions, and fluid resuscitation, respectively. Additionally, it is necessary to keep the drug induced side effects in the hemodynamic system, respiratory system, and renal system of the patient within the safe limits. Since, most of the anesthetic and analgesic drugs have respiratory and hemodynamic effects, the proposed nonovershooting controller design strategy regulates the drug administration without any overshoot, which minimizes its side effects on other vital parameters, and hence, can contribute to the development of patient safe closed-loop controllers. Moreover, since the controller aims to track desired outputs, effects of drug interactions are addressed in a systematic way.

Even though the proposed controller exhibits promising performance for the 10 patients considered with different pharmacokinetic and pharmacodynamic parameters, it is recommended to categorize patients with similar pharmacokinetic and pharmacodynamic parameters and design controllers for each patient group. For instance, the effect-site drug concentration of anesthetic and analgesic drugs that can cause 50% drug effect decreases considerably with age [50]. Hence, designing different controllers for different age groups such as infants, young adults, and elderly patients is desirable.

Finally, we used a hybrid extended Kalman filter as a standard approach for state estimation of nonlinear systems. Our assumption here is that the measurement noise has a Gaussian distribution and the nonlinear measured variables BIS(t), $t \geq 0$, and EMG(t), $t \geq 0$, can be accurately approximated locally by a linear model. However, there exists contradicting reports on the Gaussianity of EEG activity [51]. Hence, studying the efficacy of a nonlinear state estimator such as a particle filter, which can account for measurement noise with a non-Gaussian distribution as well as high-order nonlinearities can be considered as part of future work.

All these challenges should be accounted for when designing the closed-loop controller for combined administration of anesthetics and analgesics. We have not considered these factors in our design due to the lack of an adequate mathematical model that captures all such characteristics. Further research is needed to derive adequate models for anesthesia and analgesia which will help in testing and validating closed-loop strategies for anesthesia and analgesia administration. Moreover, it is important to extend the proposed controller design method to account for input constraints and time delays associated with the closed-loop control of anesthesia administration.

5. Conclusions

In this paper, a nonovershooting controller for the simultaneous infusion of sedatives and analgesics is proposed. Simulation results using 20 patients with varying pharmacokinetic and pharmacodynamic parameters show that the proposed nonovershooting controller design method is promising. Our simulation results show that the nonovershooting controller can achieve robustness to system parameter uncertainties. Further investigation of the performance of such controllers along with more precise analgesic models that can account for the strength of the pain causing stimuli and endogenous pain reduction mechanism is required. Finally, including additional vital physiological parameters such as heart rate and respiratory rate in the controller design will be considered as a part of future research direction for this work.

References

[1] J. Jacobi, G.L. Fraser, D.B. Coursin, R.R. Riker, D. Fontaine, E.T. Wittbrodt, D.B. Chalfin, M.F. Masica, H.S. Bjerke, W.M. Coplin, D.W. Crippen, B.D. Fuchs, R.M. Kelleher, P.E. Marik, S.A. Nasraway, M.J. Murray, W.T. Peruzzi, P.D. Lumb, Clinical practice guidelines for the sustained use of sedatives and analgesics in the critically ill adult, ASHP Therapeutic Guidelines, Am. J. Health-Syst. Pharm. 59 (2002) 150–178.
[2] J.P. Van Den Berg, H.E.M. Vereecke, J.H. Proost, D.J. Eleveld, J.K.G. Wietasch, A.R. Absalom, M.M. Struys, Pharmacokinetic and pharmacodynamic interactions in anaesthesia. A review of current knowledge and how it can be used to optimize anaesthetic drug administration, BJA: Br. J. Anaesth. 118 (1) (2017) 44.
[3] C.M. Ionescu, I. Nascu, R. De Keyser, Lessons learned from closed loops in engineering: towards a multivariable approach regulating depth of anaesthesia, J. Clin. Monitor. Comput. 28 (6) (2014) 537–546.
[4] A.R. Absalom, V. Mani, T. Smet, M.M. Struys, Pharmacokinetic models for propofol defining and illuminating the devil in the detail, Br. J. Anaesth. 103 (1) (2009) 26–37.
[5] A.R. Absalom, R.D. Keyser, M.M. Struys, Closed-loop anesthesia: are we getting close to finding the holygrail? Anesth. Analg. 112 (3) (2011) 516–518.
[6] B. Marsh, M. White, N. Morton, G.N. Kenny, Pharmacokinetic model driven infusion of propofol in children, Br. J. Anesth. 67 (1991) 41–48.
[7] J.W. Johansen, P.S. Sebel, T. Smet, M.M. Struys, Development and clinical application of electroencephalographic bispectrum monitoring, Anesthesiology 93 (2000) 1336–1344.
[8] J.C. Drummond, Monitoring depth of anesthesia: with emphasis on the application of the bispectral index and the middle latency auditory evoked response to the prevention of recall, Anesthesiology 93 (2000) 876–882.
[9] S. Mehta, L. Burry, S. Fischer, J.C.M. Motta, D. Hallet, D. Bowman, C. Wong, M.O. Meade, T.E. Stewart, D.J. Cook, Canadian survey of the use of sedatives, analgesics, and neuromuscular blocking agents in critically ill patients, Crit. Care Med. 34 (2) (2006) 374–380.
[10] B. Gholami, W.M. Haddad, A.R. Tannenbaum, Relevance vector machine learning for neonate pain intensity assessment using digital imaging, IEEE Trans. Biomed. Eng. 57 (6) (2010) 1457–1466.
[11] X. Jin, C.S. Kim, G.A. Dumont, J.M. Ansermino, J.O. Hahn, Semi-adaptive feedback control of opioid infusion, 2016 American Control Conference (ACC), July (2016) 2199–2204.
[12] B. Gholami, W.M. Haddad, A.R. Tannenbaum, Agitation and pain assessment using digital imaging, Engineering in Medicine and Biology Society, Annual International Conference of the IEEE (2009) 2176–2179.
[13] H. Storm, Changes in skin conductance as a tool to monitor nociceptive stimulation and pain, Curr. Opin. Anaesthesiol. 21 (2008) 796–804.

[14] W.M. Haddad, V. Chellaboina, Stability and dissipativity theory for nonnegative dynamical systems: a unified analysis framework for biological and physiological systems, Nonlinear Anal.: Real World Appl. 6 (2005) 35–65.
[15] A.U. Schubert, M. Janda, O. Simanski, J. Bajorat, B. Pohl, R. Hofmockel, B. Lampe, A fuzzy system for regulation of the analgesic remifentanil during general anaesthesia, 16th Med Conf Contr and Autom, Ajaccio, France, June (2008) 1634–1639.
[16] C. Minto, T. Schnider, T. Short, K. Gregg, A. Gentilini, S. Shafer, Response surface model for anesthetic drug interactions, Anesthesiology 92 (2000) 1603–1616.
[17] M.W. Jann, Clinically significant interactions with anesthetic agents, in: Applied Clinical Pharmacokinetics and Pharmacodynamics of Psychopharmacological Agents, Springer, 2016.
[18] M. Mahfouf, C.S. Nunes, D.A. Linkens, J.E. Peacock, Modelling and multivariable control in anaesthesia using neural-fuzzy paradigms: Part II. Closed-loop control of simultaneous administration of propofol and remifentanil, Artif. Intell. Med. 35 (3) (2005) 207–213.
[19] R. Padmanabhan, N. Meskin, W.M. Haddad, Reinforcement learning-based control for combined infusion of sedatives and analgesics, in: 4th International Conference on Control, Decision and Information Technologies (CoDIT'17), Barcelona, Spain, April 5–7, 2017, pp. 0505–0509.
[20] R. Padmanabhan, N. Meskin, W.M. Haddad, Direct adaptive disturbance rejection control for sedation and analgesia, in: Middle East Conference on Biomedical Engineering, Doha, Qatar, February, 2014, pp. 175–179.
[21] M.J. Yun, Y.H. Kim, Y.K. Go, J.E. Shin, C.G. Ryu, W. Kim, N.J. Paik, M.K. Han, S.H. Do, W.S. Jung, Remifentanil attenuates muscle fasciculations by succinylcholine, Yonsei Med. J. 51 (4) (2010) 585–589.
[22] H. Kang, Intraoperative nociception monitoring, Anesth. Pain Med. 10 (4) (2015) 227–234.
[23] A. Chevalier, D. Copot, C.M. Ionescu, J.A.T. Machado, R. De Keyser, Emerging Tools for Quantifying Unconscious Analgesia: Fractional-Order Impedance Models, Springer International Publishing, 2014.
[24] M. Gruenewald, C. Ilies, Monitoring the nociception-anti-nociception balance, Best Pract. Res. Clin. Anaesthesiol. 27 (2) (2013) 235–247.
[25] A. Shander, F. Qin, H. Bennett, Prediction of postoperative analgesic requirements by facial electromyography during simultaneous BIS monitoring, Eur. J. Anaesthesiol. (EJA) 18 (2001) 130.
[26] R. Schmid, A. Goel, Improved tracking control in hard-disk drive servo systems: a benchmark case study, European Control Conference (ECC), June (2014) 2786–2791.
[27] R. Schmid, L. Ntogramatzidis, A unified method for the design of nonovershooting linear multivariable state-feedback tracking controllers, Automatica 46 (2) (2010) 312–321.
[28] M. Hughes, R. Schmid, Y. Tan, Implementation of a novel non-overshooting tracking control method on a LEGO robot, 2nd Australian Control Conference, Nov (2012) 289–294.
[29] C.M. Ionescu, R. De Keyser, M.M. Struys, Evaluation of a propofol and remifentanil interaction model for predictive control of anesthesia induction, 50th IEEE Conference on Decision and Control and European Control Conference (CDC-ECC) (2011) 7374–7379.
[30] F. Nogueira, T. Mendonca, P. Rocha, Positive state observer for the automatic control of the depth of anesthesia-clinical results, Comput. Methods Progr. Biomed. (2016), http://dx.doi.org/10.1016/j.cmpb.2016.08.019.
[31] W.M. Haddad, V. Chellaboina, Q. Hui, Nonnegative and Compartmental Dynamical Systems, Princeton University Press, Princeton, NJ, 2010.
[32] K. Masui, R.N. Upton, A.G. Doufas, J.F. Coetzee, T. Kazama, E.P. Mortier, M.M. Struys, The performance of compartmental and physiologically based recirculatory pharmacokinetic models for propofol: a comparison using bolus, continuous, and target-controlled infusion data, Anesth. Analg. 111 (2010) 368–379.
[33] T. Mendonca, H. Alonso, M.M. da Silva, S. Esteves, M. Seabra, Comparing different identification approaches for the depth of anesthesia using BIS measurements, IFAC Proc. Vol. 45 (16) (2012) 781–785.
[34] R.D. Keyser, D. Copot, C. Ionescu, Estimation of patient sensitivity to drug effect during propofol hypnosis, IEEE International Conference on Systems, Man, and Cybernetics, Oct (2015) 2487–2491.
[35] I. Nascu, C.M. Ionescu, I. Nascu, R. De Keyser, Evaluation of three protocols for automatic DOA regulation using propofol and remifentanil, 9th IEEE International Conference on Control and Automation (ICCA) (2011) 573–578.
[36] R. Schmid, L. Ntogramatzidis, The design of nonovershooting and nonundershooting multivariable state feedback tracking controllers, Syst. Control Lett. 61 (6) (2012) 714–722.
[37] B. Moore, On the flexibility offered by state feedback in multivariable systems beyond closed loop eigenvalue assignment, IEEE Trans. Autom. Control 21 (5) (1976) 689–692.
[38] R.E. Kalman, A new approach to linear filtering and prediction problems, J. Basic Eng. 82 (1) (1960) 35–45.
[39] D. Simon, Optimal State Estimation: Kalman, H Infinity, and Nonlinear Approaches, Wiley-Interscience, 2006.
[40] L. Ntogramatzidis, J.-F. Trégouët, R. Schmid, A. Ferrante, Globally monotonic tracking control of multivariable systems, IEEE Trans. Autom. Control 61 (9) (2016) 2559–2564.
[41] K. Soltesz, G.A. Dumont, J.M. Ansermino, Assessing control performance in closed-loop anesthesia, 21st Mediterranean Conference on Control and Automation, June (2013) 191–196.
[42] B.L. Moore, L.D. Pyeatt, V. Kulkarni, P. Panousis, A.G. Kevin, Doufas, Reinforcement learning for closed-loop propofol anesthesia: a study in human volunteers, J. Mach. Learn. Res. 15 (2014) 655–696.
[43] T.W. Bouillon, J. Bruhn, L. Radulescu, C. Andresen, T.J. Shafer, C. Cohane, S.L. Shafer, Pharmacodynamic interaction between propofol and remifentanil regarding hypnosis, tolerance of laryngoscopy, bispectral index, and electroencephalographic approximate entropy, Anesthesiology 100 (6) (2004) 1353–1372.
[44] B. Heyse, T. De Smet, M. Neckebroek, K. Van Den Hauwe, S. Bonte, E. Mortier, M. Struys, Accuracy and clinical feasibility of a new Bayesian-based closed-loop control system for propofol administration using the BIS as a controlled variable, Acta Anaesthesiol. Belg. 59 (2) (2008) 111.
[45] A.R. Absalom, G. Kenny, Closed-loop control of propofol anaesthesia using bispectral index: performance assessment in patients receiving computer-controlled propofol and manually controlled remifentanil infusions for minor surgery, Br. J. Anaesth. 90 (6) (2003) 737–741.
[46] A.R. Absalom, K.P. Mason, Total Intravenous Anesthesia and Target Controlled Infusions: A Comprehensive Global Anthology, Springer, 2017.
[47] S.E. Kern, G. Xie, J.L. White, T.D. Egan, A response surface analysis of propofol-remifentanil pharmacodynamic interaction in volunteers, J. Am. Soc. Anesthesiol. 100 (6) (2004) 1373–1381.
[48] D.P. Wibowo, S. Asad, F. Suhadi, I.W. Suranadi, I. Patellongi, I. Yusuf, M.R. Ahmad, S.K. Arif, A.H. Tanra, The analysis of prostaglandin E2 (PGE2), pain pressure threshold (PPT), and critical-care pain observation tools (CPOT) of systemic inflammatory responses syndrome (SIRS) patients in intensive care unit, Am. J. Med. Biol. Res. 5 (2) (2017) 13–17.
[49] Z.S. Messieha, S. Guirguis, S. Hanna, Bispectral index monitoring (BIS) as a guide for intubation without neuromuscular blockade in office-based pediatric general anesthesia: a retrospective evaluation, Anesth. Prog. 58 (1) (2011) 3–7.
[50] J. Barr, K. Zomorodi, E.J. Bertaccini, S.L. Shafer, E. Geller, A double blind randomised comparison of IV lorazepam versus midazolam for sedation of ICU patients via a pharmacologic model, Anesthesiology 95 (2001) 286–298.
[51] J.A. McEwen, G.B. Anderson, Modeling the stationarity and gaussianity of spontaneous electroencephalographic activity, IEEE Trans. Biomed. Eng. 22 (5) (1975) 361–369.